Dynamic Article Links ▶

PAPER

Particle nanosomes with tailored silhouettes†

Claudia S. Wagner,[a] **Andrea Fortini,**[b] **Eddie Hofmann,**[a] **Thomas Lunkenbein,**[c] **Matthias Schmidt**[b] **and Alexander Wittemann***[a]

The interest in hollow structures with defined porosities has promoted the fabrication of colloidosomes, *i.e.* capsules from spherical colloids. The hierarchically organized architectures were built from microparticles or multiple layers of nanoparticles to make sure that the capsule walls were sufficiently robust. Herein, we present for the first time a strategy towards submicron-sized capsules with walls that consist of a single layer of nanoscopic inorganic constituents. Nanoparticles and oppositely charged polymer colloids were joined at the surface of evaporating emulsion droplets. The heteroaggregates exhibited well-defined core–shell morphologies, with clusters of the polymer colloids as the core and a dense monolayer of nanoparticles as the shell. Various complex yet well-defined global shapes can be obtained in respect to the number of polymer particles. Subsequent removal of the polymer core led to capsules, which exhibited regular compartmentalized shapes. A high density of nanopores was obtained on objects with dimensions of less than half a micron. Regardless of the fact that the capsules consisted of a single layer of nanoparticles with tiny contacts keeping them together, they did not collapse or break apart. Monte Carlo computer simulations demonstrated that the nanoscopic constituents can be trapped into structurally arrested states.

1. Introduction

The current focus in nanoscience shifts from the bare synthesis of nanoparticles to their assembly into hierarchically organized materials, which are of potential interest for functional devices.[1] Many applications rely not solely on the properties of the individual building blocks but on their arrangement and interactions, which significantly determine mechanical, optical, electronic, and magnetic properties.

Joining particles that are confined onto emulsion droplets has proven to be a powerful strategy towards a plenitude of supracolloidal structures.[2–4] Emulsions stabilized by solid particles are often referred to as Pickering emulsions.[5] The adsorption of a particle at the interface results in a decrease of the total free energy, which scales with the square of the particle radius.[6] Particles with dimensions of several tens of nanometres are efficiently confined at the droplet surface because their adsorption energy largely exceeds the thermal energy. Moreover, when monomers are used as the dispersed phase, polymerization of the particle-coated droplets results in raspberry-like colloids.[7]

Gentle evaporation of the dispersed phase in a Pickering emulsion induces agglomeration of the solid particles into supracolloidal assemblies. Depending on the density of particles, clusters with a small number of constituents,[2,8] compact supra-balls made from a large number of individual particles,[9] or hollow microcapsules[10] were obtained. The latter are often termed "colloidosomes", in analogy to liposomes.[11] The wall of the capsules consisted either of a densely packed monolayer of microparticles[10–13] or of multilayers of nanoparticles.[14–16] The stability of the walls stems from van der Waals forces and from hydrophobic interactions.[10,14] It can be strengthened by thermal sintering,[12,15] gelation of the internal phase[17] or by cementing the particles.[18] Alternatively, the particles can be linked by covalent bonds.[19,20] The porosity of the capsules and, as a consequence, their permeability, specific surface area and optical properties can be precisely tailored by the size and interfacial properties of the constituent particles.[12,21] This opens up perspectives for delivery and controlled release of active ingredients, applications in catalysis and photonics, as well as for use as microscale reaction vessels.[20] Hollow structures of spherical particles were also prepared by adsorption of inorganic particles onto polystyrene or carbon microspheres, occasionally inter-locking the adsorbed particles by coating with silica, and subsequent removal of the organic carrier by pyrolysis.[22]

Both fluid and solid supports for particles tend to be spherical because minimization of surface tension favors spherical

[a]Physikalische Chemie I, Universität Bayreuth, Universitatsstr. 30, D-95440 Bayreuth, Germany. E-mail: alexander.wittemann@uni-bayreuth.de
[b]Theoretische Physik II, Physikalisches Institut, Universität Bayreuth, Universitatsstr. 30, D-95440 Bayreuth, Germany
[c]Anorganische Chemie I, Universität Bayreuth, Universitatsstr. 30, D-95440 Bayreuth, Germany
† Electronic supplementary information (ESI) available: Distribution of the heterocomposites as measured by disk centrifugal sedimentation; movie showing the temporal evolution of the equilibration of a simulated tetrahedral nanosome. See DOI: 10.1039/c1sm07014b

geometries. For this reason, the majority of colloidosomes reported in the literature exhibits spherical shapes. A higher level of complexity can be obtained by accumulating particles within double emulsion droplets. This allowed the preparation of nonspherical colloidosomes that possess several open compartments.[23] Similar structures were obtained by selective removal of the larger constituents of binary heterocomposite particles. This approach allowed the preparation of structures with coordinated notches[3,16] or closed capsules,[16] depending on the morphology of the heterocomposites. In all these cases, the walls of the nonspherical colloidosomes are made up of multiple layers of nanoparticles.

Here we present for the first time a strategy towards submicron-sized nonspherical capsules with walls that consist of a single layer of nanoparticles. In this approach, the silhouettes of the capsules can be precisely engineered via a specific number of "sacrificial" colloids, which determine the global shape of the nanoparticle assemblies. Central questions that we addressed using experiments and Monte Carlo (MC) simulations were (i) in which manner the sacrificial colloids organize the nanoparticles and (ii) whether or not stable nanoparticle assemblies can be obtained after removal of the templating colloids.

We term the resulting capsules "particle nanosomes" rather than "colloidosomes" to emphasize the smaller dimensions of the constituents, and the substantially smaller porosity of such containers, which offers perspectives for the retarded release of nanosized actives.

2. Materials and methods

2.1 Materials

Silica nanoparticles (Ludox TMA) were purchased from Sigma and purified by exhaustive dialysis against water (Millipore Academic A10). The synthesis and purification of the cationic PS particles are described in ref. 8.

2.2 Methods

2.2.1 Field emission scanning electron microscopy. Micrographs were taken on a Zeiss LEO 1530 Gemini microscope equipped with a field emission cathode operating at 4 kV. Specimen preparation was performed along the lines given in ref. 24.

2.2.2 Transmission electron microscopy. Specimens were prepared by placing minute amounts of 0.05 wt% suspensions onto a grid (Plano SiMPore UltraSM®) coated with a non-porous silicon film that can withstand temperatures of up to 600 °C in air. After 2 minutes, excess liquid was removed. The transmission electron microscope (Zeiss EM 922 EFTEM) was operated at an acceleration voltage of 200 kV. All images were recorded digitally by a bottom-mounted 16 bit CCD camera system (Gatan Ultra-Scan 1000). Images were processed with a digital imaging processing system (Gatan Digital Micrograph 3.9).

2.2.3 Zeta potential measurements. Electrophoretic mobilities of the PS particles and the silica nanoparticles were measured on a Malvern Zetasizer Nano ZS. The ionic strength was fixed by addition of NaCl to 10^{-4} M. Because the radii a of the particles are of similar magnitude as the Debye length

$\kappa^{-1} = 30.4$ nm, the mobilities were converted into zeta potentials ζ using the approximation of Henry's formula by Oshima to ensure validity for all values of κa.[25]

2.3 Theoretical modeling and simulations

Recently, a mechanism to intrinsically stabilize hollow shells composed of individual particles was explored by Monte Carlo simulations.[26] It was found that the interplay of attractive and repulsive interactions can provide energy barriers, which are sufficiently large to dynamically lock the particles and stabilize the shells. Based on this concept, we studied N_n nanoparticles with hard-sphere diameter σ_n that were adsorbed on a cluster of N_c colloids, each with hard-sphere diameter $\sigma_c = 7.8\sigma_n$. The interaction between two nanoparticles at distance r is

$$\varphi_{nn}(r) = \begin{cases} \infty & r < \sigma_n \\ -\varepsilon_{sw} & \sigma_n \leq r < r_{sw} \\ \varepsilon_{nn}\, e^{-\kappa_{nn}(r-\sigma_n)}/r & \text{otherwise,} \end{cases}$$

with $r_{sw} = 1.1\sigma_n$ being the range of an attractive square well of depth $\varepsilon_{sw} = 9k_B T$, where k_B is the Boltzmann constant and T is the temperature. The parameter $\varepsilon_{nn} = 25k_B T$ is the contact value of the long-ranged repulsive Yukawa interaction with inverse Debye length $\kappa_{nn} = 10\sigma_n^{-1}$. The interaction between nanoparticles and each colloid was taken to be a hard-core repulsion and an attractive Yukawa well,

$$\varphi_{nc}(r) = \begin{cases} \infty & r < 0.5(\sigma_n + \sigma_c) \\ -\varepsilon_{nc}\, e^{-\kappa_{nc}[r-(\sigma_n+\sigma_c)/2]}/r & 0.5(\sigma_n + \sigma_c) \leq r < r_{cut} \\ 0 & \text{otherwise,} \end{cases}$$

with $\kappa_{nc} = 3\sigma_n$, $\varepsilon_{nc} = 80k_B T$ and $r_{cut} = 0.75\sigma_n + 0.5\sigma_c$.

The colloids were initialized in a cluster configuration and were used as templates for the nanoparticles. These were initialized on the cluster surface by RSA,[27] which was stopped when the value $N_n = 70N_c$ was reached.

We carried out Metropolis Monte Carlo (MC) simulations. Here the nanoparticles moved with a maximum MC trial displacement $0.01\sigma_n$. At every N_n sweep, an attempt to shrink or increase the diameter of the big particles by a maximal amount of $0.01\sigma_n$ was made. The shrinking rate was governed by an external pressure $P = 6k_B T\sigma_n^{-3}$ that acted on the clusters in a constant pressure MC scheme. The relative distances between the colloids in the clusters were also rescaled, while the nanoparticle positions were not changed in this move. The shrinking process was carried out for 10^7 MC sweeps. In order to check for the stability of the nanoparticle shells we removed the template and ran simulations for 10^7 MC sweeps on the free nanosome structure with a constant volume MC scheme.

3. Results and discussion

Scheme 1 outlines the fabrication of particle nanosomes, which consisted of two consecutive steps: at first, 33 nm sized (diameter) negatively charged silica particles and 154 nm sized positively charged polystyrene particles (Scheme 1A) were joined via the emulsion droplet process.[8] The resulting heterocomposites exhibited core–shell morphologies, with clusters of PS particles as the core and a dense monolayer of the silica nanoparticles as
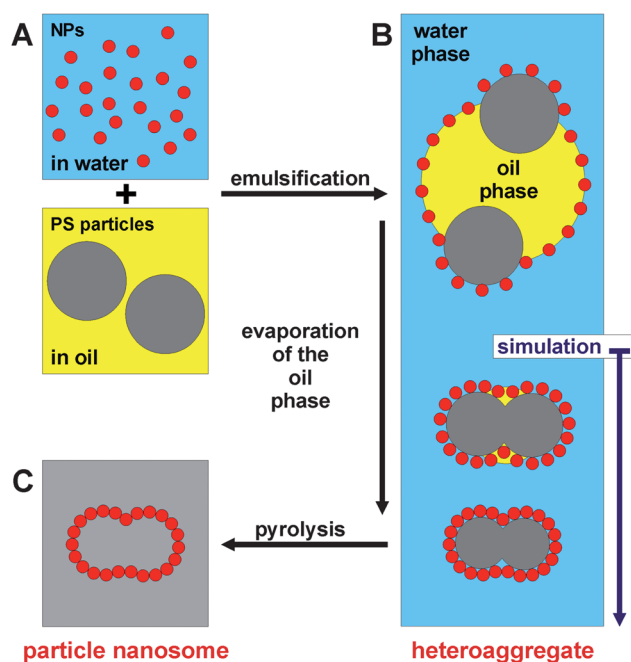
Scheme 1 Illustration of the strategy towards particle nanosomes (A → C): emulsion droplets served as templates which allow for controlled joining of oppositely charged inorganic nanoparticles and polymer colloids (A). Segregation of the particles during droplet evaporation-driven assembly resulted in defined hybrid composites with the nanoparticles organized into a closed monolayer surrounding a complex core composed of the colloids (B). Hollow capsules with high porosity and regular shapes were obtained after removal of the core (C). See text for further explanation.

the shell (Scheme 1B). Subsequent removal of the polymer core led to nanoporous silica capsules (Scheme 1C).

In detail, 92 mg anionic silica nanoparticles (zeta potential $\zeta = -78 \pm 5$ mV) were dispersed in 27 ml water. The aqueous suspension was gently covered with 3 ml of toluene, in which 74 mg of amine-modified cross-linked PS particles ($\zeta = +92 \pm 5$ mV) were dispersed. On average 59 silica nanoparticles per PS sphere were added. In doing so, the oppositely charged particles were kept in different phases to ensure that they could exclusively interact at the oil–water interface. If oppositely charged particles are brought together within the same phase, fractal aggregates are usually obtained in the dilute regime.[28] One viable solution to circumvent this is the use of a solvent that moderates the interactions among the particles. This allowed the production of ionic colloidal crystals.[29] In contrast, in the present study uncontrolled aggregation is suppressed by shifting the assembly to the oil–water interface.

Emulsification into narrowly dispersed microdroplets was accomplished by sonication using a high-shear device (Bandelin Sonoplus HD 3200, probe KE 76) along the lines described recently.[4] Because of the Pickering effect, the PS particles were firmly bound to the oil–water interface. Nonetheless, they could still diffuse at the droplet surface.[30]

The silica nanoparticles were added *via* the aqueous phase. For this reason, they could adhere on the droplets, but they could also adsorb directly onto the oppositely charged PS particles. Obviously, adsorption onto the PS particles is restricted to the sides that are exposed to the aqueous phase (Scheme 1B).

Because toluene is a good solvent for polystyrene, the cross-linked PS spheres were swollen with the dispersed toluene while bound onto the droplet. Dynamic light scattering experiments revealed a hydrodynamic diameter of the PS particles in toluene of 260 nm, which is significantly larger than their diameter in water (154 nm). Hence, during adsorption of the silica nanoparticles the diameter of the polymer particles significantly exceeded their solid diameter. The adsorption of the nanoparticles onto the PS surface is governed by the electrostatic attraction towards the PS surface and the repulsion among the nanoparticles, resulting in a coverage that is below the limit expected for random sequential adsorption (RSA) of hard spheres, *i.e.* 54.7%.[31] This is corroborated by a recent study on the adsorption of silica nanoparticles onto solid PS particles.[24]

The assembly into heterocomposites was induced by gentle removal of the dispersed phase (Scheme 1B). This was accomplished by evaporation of toluene under reduced pressure using a rotary evaporator. The evaporation of toluene is accompanied by a decrease of the size of the PS particles towards their solid diameter. This causes packing of the nanoparticles which have been already adsorbed onto the PS surface. Moreover, the nanoparticles at the oil–water interface are gradually deposited onto the PS particles as the droplet surface decreases. Hence, a closed layer of nanoparticles was obtained, which completely covered the assembly of PS particles, resulting in nanoparticle-encased PS clusters.

The left column of Fig. 1 presents field emission scanning electron micrographs of the composites. Complementary information on the assemblies was obtained by transmission electron microscopy (Fig. 2A). Furthermore, the distribution of the composites was measured by differential centrifugal sedimentation (CPS Instruments CPS-24000). All methods clearly demonstrate that the organization of the PS particles into clusters determines the global shapes of the composites with the silica nanoparticles deposited onto the surface of the PS clusters. The configurations of the PS clusters found in electron micrographs are identical to those found in the absence of nanoparticles.[4,30] Moreover, fractionation of the composites follows the numbers of the PS constituents during differential centrifugal sedimentation measurements (see Fig. S1 in the ESI†). This makes the PS particle doublets, triplets, tetrahedral, triangular dipyramids, *etc.* act as a complex template for the deposition of nanoparticles. As a result a closely packed monolayer of silica particles covered the PS clusters.

The organization of the nanoparticles onto the polymer particles was explored by MC computer simulations. For the sake of simplicity, in simulations we regarded the adsorption of small spheres onto individual clusters pre-formed from two to seven larger spheres. The uptake of the small spheres was initialized by random sequential adsorption onto swollen clusters.[27] Subsequently, the clusters were shrunk gradually. The shrinkage modeled the late stage of the formation of the composites, with the PS particles already touching each other while still swollen with the dispersed phase (Scheme 1B). The interaction among the charged nanoparticles was described by a long-ranged repulsive Yukawa potential in combination with a short-ranged square-well attraction, in order to mimic the van
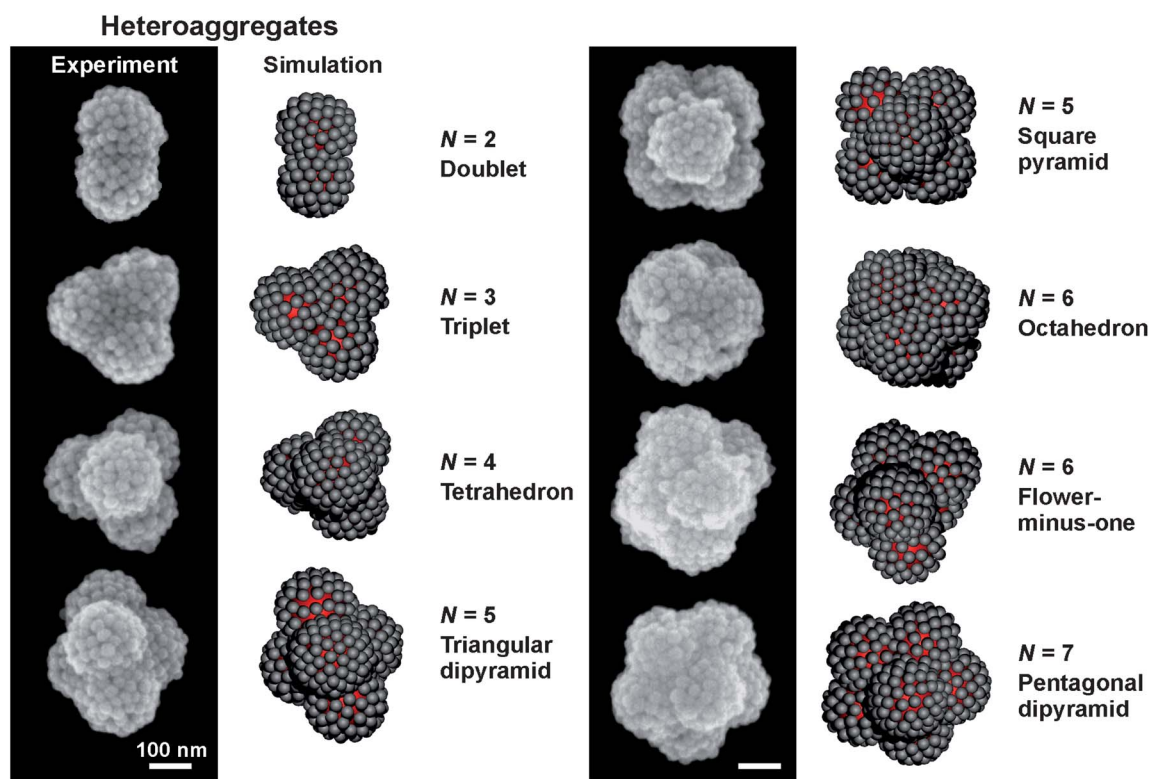
Fig. 1 Synopsis of heterocomposites from positively charged PS particles and negatively charged silica nanoparticles. The co-assembly of both types of particles moderated by emulsion droplets resulted in well-defined morphologies with the number of PS particles N determining the global shape of the heteroaggregates. FESEM micrographs (first and third column) demonstrate the formation of a closed single layer of nanoparticles which encased the PS particles that organized into clusters of specific configurations. MC simulations (second and fourth column) attribute the dense packing of nanoparticles to gradual compaction of an initially randomized adsorption.
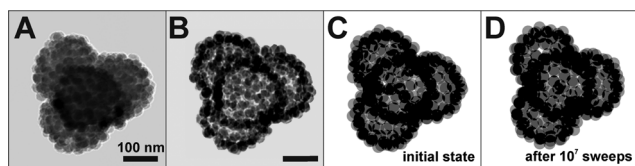

Fig. 2 Towards robust nanoporous structures: (A) TEM micrograph of a tetrahedral heteroaggregate; (B) the increase in transmission after pyrolysis indicates the removal of the complex PS core; (C) simulation snapshot of a tetrahedral nanosome (without inner template) in transmission mode, *i.e.* semi-transparent spheres were used to represent the nanoparticles in order to simulate the TEM micrograph shown in (B); and (D) the marginal differences after 10^7 MC sweeps demonstrate that kinetically stable nanoparticle capsules could be obtained.

der Waals interactions. Therefore, the nanoparticles could irreversibly coagulate if their distance got small enough to overcome the repulsive energy barrier. Because of the pronounced net charge of the oppositely charged colloids modeled as an attractive Yukawa potential, the nanoparticles were strongly attracted by the clusters, resulting in practically irreversible binding. The right columns of Fig. 1 show snapshots of equilibrium configurations after 10^7 MC sweeps.

The FESEM micrographs (left columns in Fig. 1) show a dense packing of the silica particles on the PS surface. However, their organization is substantially different from that in a hexagonally packed layer. This is corroborated by the MC simulations, which indicate disordered packing of the nanoparticles, resulting in structural defects within the jammed state. The voids found in simulations resemble those observed in the micrographs (Fig. 1). However, the voids hardly resulted in uncovered surface areas, indicated in red in Fig. 1, given that enough silica particles were added to form a dense layer. It was found in the experiments that a ratio of silica nanoparticles per PS sphere of 59 : 1 is best suited to get monolayer coverage. Higher ratios of silica nanoparticles resulted in free particles left in solution. On the other hand, lower ratios resulted in only partial coverage of the PS surface. In the simulations the number of nanoparticles for monolayer coverage was chosen slightly higher (70 : 1) than the experimental value to take the larger surface of the idealized colloidal clusters into account. The smaller surface area of the experimental clusters stems from partial fusion between the PS particles during their assembly at the oil–water interface.[32]

Weitz and co-workers studied PS microspheres that were adsorbed onto oppositely charged thermosensitive microgels.[33] Thermally induced shrinkage of the gel particles forced the PS microspheres to pack into a jammed state. Further shrinkage resulted in concomitant buckling of the PS particle shells. Interestingly, we found only moderate buckling of the shells. The nanoparticles were slightly squeezed out of the densely packed monolayer during shrinkage of the polymer particles upon evaporation of toluene. This can be seen in the FESEM

micrographs and is reproduced well in the simulations (right column in Fig. 1).

We fabricated nanoparticle capsules by removal of the PS core through pyrolysis (Fig. 2). This was accomplished by gradual heating of the composites (rate 10 °C min⁻¹) to 500 °C and maintaining this temperature for 60 min. TEM micrographs of the resulting structures showed a marked increase in transmission after the thermal treatment, pointing to the formation of hollow structures (Fig. 2). Fourier transform infrared spectra demonstrated that the polystyrene was completely decomposed. Elemental analysis (Vario elementar EL III-CHN) was carried out to detect if any carbon was left over. Before pyrolysis, a carbon content of 40.2% was found for the composites, which corresponds to 58 silica nanoparticles per PS sphere. This is in good agreement with the ratio of particles added (59 : 1) conforming the validity of the method. Elemental analysis after pyrolysis demonstrated complete removal of the polymer. Only minute traces of carbon (0.1%) were detected.

Fig. 3 shows a survey of nanosomes with various shapes. An important feature of the nanosomes is the connectedness of their inner compartments, which allows free circulation of encapsulated actives. Despite the rather harsh thermal treatment, all electron micrographs clearly showed that the nanoparticle shells remained intact. This is remarkable inasmuch as the shells consisted of a single layer of particles with few van der Waals contacts that keep the shell together. Baking together of the particles is not likely to happen because the temperature during pyrolysis (500 °C) was considerably lower than the sintering temperature of silica nanoparticles (>600 °C).[34] This was corroborated by krypton sorption at 77 K, which revealed that the specific surface areas of the individual silica particles and the nanosomes are identical (94 m² g⁻¹) within the limits of experimental error. Hence, only incipient sintering might occur.

For this reason, interactions within the nanoparticle capsules are widely reduced to a combination of short-range attraction and long-range repulsion between the nanoparticles after removal of the cluster core. As shown in simulations single-layered nanoparticle capsules inevitably collapse, when the attraction dominates over the repulsion. Conversely, when the relative strength of the repulsion largely exceeds the attractive interactions, the capsules burst.[26] Hence, the competing interactions have to be adequately balanced to obtain kinetically stable nanosomes. This could be hampered by their complex shapes with many indentations that could trigger local rearrangement of the nanoparticles.[35] For this reason, we checked the thermal stability with MC simulations by performing additional 10⁷ MC sweeps for various types of capsule configurations after removal of the inner core. Remarkably, we found cases where the capsules remained stable over the long run time, even though the parameters were not optimized. Hence, the interplay among attraction and repulsion prevented the nanoparticles from both agglomerating and escaping from the shell although the nanosomes were thermodynamically not in equilibrium (Fig. 2D and see Movie in the ESI†). Moreover, the simulation runs in which the capsules collapsed or broke apart clearly demonstrated that the necks between the compartments are not the source of instability, which demonstrated that stability and complexity of the nanoparticle shells were not mutually exclusive. Hence, the simulations showed that the associated energy barriers can be
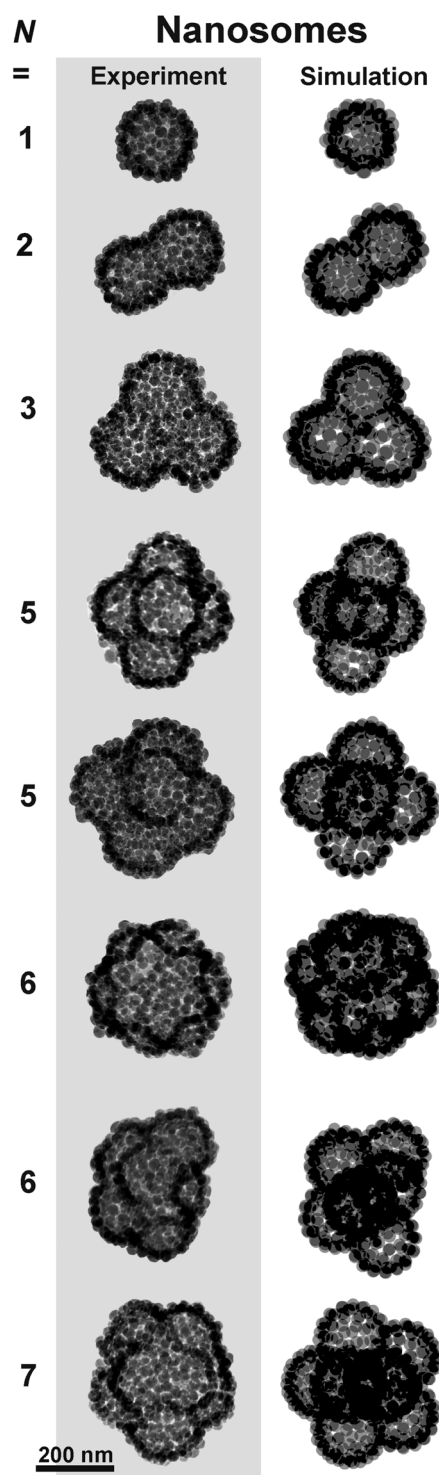

Fig. 3 Overview of experimental nanosomes (left column: TEM micrographs) and their theoretical counterparts (right column: MC simulations). *N* denotes the number of sacrificial colloids that governed the shape of the nanoporous capsules.

sufficiently large for trapping the nanoparticles into structurally arrested states. These results are qualitatively consistent with the stability phase diagram of ref. 26; a more detailed comparison is not possible at this stage because of different values of the simulation parameters.

4. Conclusions

We presented a strategy towards nanoporous colloidal capsules. Diverse shapes can be obtained with the help of "sacrificial" colloids that determine the organization of nanoparticles. Albeit the walls consisted of a single layer of inorganic nanoparticles, stable hierarchically organized structures can be obtained. The approach is quite versatile because it can be used for a broad range of inorganic nanoparticles opening unprecedented perspectives for designer capsules. Combination of different types of nanoparticles within the monolayer shells would allow implementing multifunctionality and even the generation of barcode hollow structures with nanoscale resolution. Beyond this, a high density of nanopores is realized on capsules with dimensions of less than 500 nm. In this regard, they mimic compartmentalized systems in biology such as cells or organelles. Future challenges to exploit the full potential of nanosomes are to produce them at larger scales, to transfer them into solution, and to study the uptake and release kinetics of actives.

Notes and references

1 E. W. Edwards, D. Wang and H. Moehwald, *Macromol. Chem. Phys.*, 2007, **208**, 439; A. B. Pawar and I. Kretzschmar, *Macromol. Rapid Commun.*, 2010, **31**, 150.
2 V. N. Manoharan, M. T. Elsesser and D. J. Pine, *Science*, 2003, **301**, 483.
3 Y.-S. Cho, G.-R. Yi, S.-H. Kim, S.-J. Jeon, M. T. Elsesser, H. K. Yu, S.-M. Yang and D. J. Pine, *Chem. Mater.*, 2007, **19**, 3183.
4 C. S. Wagner, B. Fischer, M. May and A. Wittemann, *Colloid Polym. Sci.*, 2010, **288**, 487.
5 B. P. Binks and M. Kirkland, *Phys. Chem. Chem. Phys.*, 2002, **4**, 3727.
6 P. Pieranski, *Phys. Rev. Lett.*, 1980, **45**, 569.
7 F. Tiarks, K. Landfester and M. Antonietti, *Langmuir*, 2001, **17**, 5775; A. Schmid, S. P. Armes, C. A. P. Leite and F. Galembeck, *Langmuir*, 2009, **25**, 2486.
8 C. S. Wagner, Y. Lu and A. Wittemann, *Langmuir*, 2008, **24**, 12126.
9 S.-H. Kim, S. Y. Lee, G.-R. Yi, D. J. Pine and S.-M. Yang, *J. Am. Chem. Soc.*, 2006, **128**, 10897.
10 O. D. Velev, K. Furusawa and K. Nagayama, *Langmuir*, 1996, **12**, 2374.
11 A. D. Dinsmore, M. F. Hsu, M. G. Nikolaides, M. Marquez, A. R. Bausch and D. A. Weitz, *Science*, 2002, **298**, 1006.
12 H. N. Yow and A. F. Routh, *Langmuir*, 2009, **25**, 159.
13 N. P. Ashby, B. P. Binks and V. N. Paunov, *Phys. Chem. Chem. Phys.*, 2004, **6**, 4223.
14 D. Lee and D. A. Weitz, *Adv. Mater.*, 2008, **20**, 3498.
15 C. Yuan, Y. Xu, N. Jiang, G. Chen, B. Xu, N. He and L. Dai, *Soft Matter*, 2011, **7**, 3366.
16 S. Y. Lee, L. Gradon, S. Janeczko, F. Iskandar and K. Okuyama, *ACS Nano*, 2010, **4**, 4717.
17 H. Duan, D. Wang, N. S. Sobal, M. Giersig, D. G. Kurth and H. Moehwald, *Nano Lett.*, 2005, **5**, 949.
18 H. Wang, X. Zhu, L. Tsarkova, A. Pich and M. Moeller, *ACS Nano*, 2011, **5**, 3937.
19 H. Skaff, Y. Lin, R. Tangirala, K. Breitenkamp, A. Boeker, T. P. Russell and T. Emrick, *Adv. Mater.*, 2005, **17**, 2082; K. L. Thompson, S. P. Armes, J. R. Howse, S. Ebbens, I. Ahmad, J. H. Zaidi, D. W. York and J. A. Burdis, *Macromolecules*, 2010, **43**, 10466.
20 B. Samanta, D. Patra, C. Subramani, Y. Ofir, G. Yesilbag, A. Sanyal and V. M. Rotello, *Small*, 2009, **5**, 685.
21 R. T. Rosenberg and N. R. Dan, *J. Colloid Interface Sci.*, 2011, **354**, 478.
22 M. D'Acunzi, L. Mammen, M. Singh, X. Deng, M. Roth, G. K. Auernhammer, H.-J. Butt and D. Vollmer, *Faraday Discuss.*, 2010, **146**, 35; Y. Zhu, E. Kockrick, T. Ikoma, N. Hanagata and S. Kaskel, *Chem. Mater.*, 2009, **21**, 2547.
23 D. Lee and D. A. Weitz, *Small*, 2009, **5**, 1932.
24 C. S. Wagner, S. Shehata, K. Henzler, J. Yuan and A. Wittemann, *J. Colloid Interface Sci.*, 2011, **355**, 115.
25 H. Ohshima, *J. Colloid Interface Sci.*, 1994, **168**, 269.
26 E. Mani, E. Sanz, P. G. Bolhuis and W. K. Kegel, *J. Phys. Chem. C*, 2010, **114**, 7780.
27 *Advances in Particle Adhesion*, ed. D. S. Rimai, L. H. Sharpe, Gordon and Breach, Amsterdam, 1996.
28 J. M. Lopez-Lopez, A. Schmitt, A. Moncho-Jorda and R. Hidalgo-Alvarez, *Soft Matter*, 2006, **2**, 1025.
29 M. E. Leunissen, C. G. Christova, A.-P. Hynninen, C. P. Royall, A. I. Campbell, A. Imhof, M. Dijkstra, R. van Roij and A. van Blaaderen, *Nature*, 2005, **437**, 235.
30 I. Schwarz, A. Fortini, M. Schmidt, C. S. Wagner and A. Wittemann, *J. Chem. Phys.*, submitted.
31 Z. Adamczyk and P. Weronski, *Adv. Colloid Interface Sci.*, 1999, **83**, 137.
32 M. Hoffmann, C. S. Wagner, L. Harnau and A. Wittemann, *ACS Nano*, 2009, **3**, 3326.
33 J.-W. Kim, A. Fernandez-Nieves, N. Dan, A. S. Utada, M. Marquez and D. A. Weitz, *Nano Lett.*, 2007, **7**, 2876.
34 H. E. Bergna, in *Colloidal Silica: Fundamentals and Applications*, ed. H. E. Bergna and W. O. Roberts, CRC Press, Boca Raton, 2006.
35 G. A. Vliegenthart and G. Gompper, *New J. Phys.*, 2011, **13**, 045020.